# Adaptive model-free formation-tracking controller and observer for collaborative payload transport by drones

Ali Safaei
Dep. of Mechanical Engineering
McGill University
Montreal, Quebec
ali.safaei@mail.mcgill.ca

Inna Sharf
Dep. of Mechanical Engineering
McGill University
Montreal, Quebec
inna.sharf@mcgill.ca

***Abstract*—In this paper, a solution is provided for collaborative transportation of a rigid payload by four quadrotors, while a desired formation topology is maintained among the vehicles. Each quadrotor is connected to the payload using a rigid link, where the joints to the payload are located on two perpendicular lines through the center of mass of the payload. The proposed solution includes a control scheme comprising different modules. Each module is responsible for controlling the motion of a specific subsystem of the entire payload-links-quadrotors system. Since an adaptive model-free control algorithm is utilized for tracking the desired set-points for each module, no information on the internal dynamics of the drones is required. Moreover, by utilizing a special linear Kalman filter for estimating the unit vectors along the connecting rigid links, the requirement for position and velocity estimation of the drones is revoked. Instead, the position and velocity of the payload must be estimated by using appropriate sensors. The solution is validated via numerical simulation of transporting a payload along a time-varying trajectory.**

## I. Introduction

In recent years, a swarm of autonomous flying mobile robots has been increasingly considered as a challenging research topic, as well as a beneficial commercial product. A swarm can be used for rescue and surveillance missions, aerial video capture, agricultural applications such as harvest spraying and for aerial night shows. Another attractive application is to transport a relatively heavy payload by multiple drones in a collaborative way. To achieve collaborative payload transportation, a control scheme must be provided to ensure smooth movement of the payload, while preventing the drones from crashing into each other. In addition, considering the geometrical constraints on the system, an observer algorithm can be designed in a way so as to be implemented with fewer sensors mounted on the system. In literature, there are some investigations on transporting soft payloads [1]. Also some solutions have been proposed for transporting the payload using flexible links [2]. In this paper, we focus on transporting a rigid payload connected to drones by massless rigid links.

In [4], a control solution considering the payload dynamics is suggested, while the tension forces in the rigid links are determined using the concept of differential-flatness. In that work, no considerations are taken to a desired formation among the quadrotors. Later in [3], a cooperative consensus controller is proposed for position and velocity tracking problem of each quadrotor. A desired formation among the drones is achieved, while the payload and quadrotors are traversing at a desired velocity. The solution requires information on the internal dynamics of each quadrotor. Moreover, each quadrotor must be equipped with a precise GPS module and an observer for estimating its velocity.

The authors of [5] have designed a method based on virtual repulsive forces between two quadrotors carrying a suspended load, in order to achieve a collision-free transportation of the payload. In [6], the problem of collaborative payload transportation is solved by suggesting a link-free mechanism, where the quadrotors are directly attached to the payload. It is shown that the optimal configuration of the quadrotors is a rectangle, where each quadrotor is located at one corner of that rectangle. Obviously, this solution cannot be implemented on small-size heavy payloads.

In [7], a decentralized adaptive consensus velocity controller is designed for each quadrotor, in order to force the whole system to follow a desired velocity. In that solution, the payload mass is assumed to be unknown and an adaptive law is proposed to estimate it, on each quadrotor. Moreover, full knowledge of the internal dynamics of the quadrotors is assumed, and the availability of precise GPS module on each quadrotor is required. Furthermore in [8] and [9], a solution is provided for the collaborative payload transportation problem, by dividing the entire problem into a series of several tracking control problems. By employing proportional-derivative controllers for each of the tracking problems, and also by using a pseudo-inverse solution for the dynamics equation of the payload, a swing-free transportation of the payload is provided along a time-varying trajectory. In that solution, it is also assumed that the orientation of the links connecting the drones to the payload is known, which is not a reasonable assumption in practice. Moreover, there

is no consideration in [8] and [9] for inter-agent collision avoidance among the drones.

In light of the limitations of the previous investigations, a novel solution is provided here for the problem of payload transportation with four aerial mobile robots attached to the payload by rigid links. The proposed control and observer schemes are designed to eliminate the need for estimating position and velocity of each quadrotor. Instead, position and velocity of the payload must be measured using a sensor module attached to the payload enclosure. Therefore, contributions of the current solution are:

- an adaptive model-free control algorithm is utilized to remove the requirement for information on mass and inertia matrix of the quadrotors;
- a desired formation among the drones is maintained for collision avoidance, while transporting the payload;
- an observer is designed for estimating the orientation of the links, which eliminates the need for estimating the position and velocity of the drones.

## II. Dynamics Model

**Definition-1**. A dynamic system including four drones, four massless rigid links and a rigid payload is considered (see Fig. 1). Following [8], [9], the dynamics of such system is defined as follows

$$
\begin{aligned}
&\mathbf{M_q}(\ddot{\mathbf{p}}_o - \mathbf{G}) - \sum_{i=1}^{4}(m_i \mathbf{q}_i \mathbf{q}_i^T \mathbf{R_o} \boldsymbol{\rho}_i^{\times} \dot{\boldsymbol{\omega}}_o) = \\
&\qquad \sum_{i=1}^{4}(\mathbf{u_i^{\parallel}} - m_i l ||\boldsymbol{\omega}_i^2|| \mathbf{q_i} - m_i \mathbf{q}_i \mathbf{q}_i^T \mathbf{R_o} \boldsymbol{\omega}_o^{\times} \boldsymbol{\omega}_o^{\times} \boldsymbol{\rho}_i) \ , \\
&(\mathbf{J_o} - \sum_{i=1}^{4}(m_i \boldsymbol{\rho}_i^{\times} \mathbf{R_o}^T \mathbf{q}_i \mathbf{q}_i^T \mathbf{R_o} \boldsymbol{\rho}_i^{\times}))\dot{\boldsymbol{\omega}}_o + \\
&\qquad \sum_{i=1}^{4}(m_i \boldsymbol{\rho}_i^{\times} \mathbf{R_o}^T \mathbf{q}_i \mathbf{q}_i^T (\ddot{\mathbf{p}}_o - \mathbf{G})) + \boldsymbol{\omega}_o^{\times} \mathbf{J_o} \boldsymbol{\omega}_o = \\
&\qquad \sum_{i=1}^{4}(\boldsymbol{\rho}_i^{\times} \mathbf{R_o}^T (\mathbf{u_i^{\parallel}} - m_i l ||\boldsymbol{\omega}_i^2|| \mathbf{q_i} - m_i \mathbf{q}_i \mathbf{q}_i^T \mathbf{R_o} \boldsymbol{\omega}_o^{\times} \boldsymbol{\omega}_o^{\times} \boldsymbol{\rho}_i)) \ , \\
&\dot{\boldsymbol{\omega}}_i = \frac{1}{l} \mathbf{q_i}^{\times} (\ddot{\mathbf{p}}_o + \mathbf{G} - \mathbf{R_o} \boldsymbol{\rho}_i^{\times} \dot{\boldsymbol{\omega}}_o + \mathbf{R_o} \boldsymbol{\omega}_o^{\times} \boldsymbol{\omega}_o^{\times} \boldsymbol{\rho}_i) - \frac{1}{m_i l} \mathbf{q_i}^{\times} \mathbf{u_i^{\perp}} \ , \\
&\mathbf{J_i} \dot{\boldsymbol{\omega}}_{qi} + \boldsymbol{\omega}_{qi}^{\times} \mathbf{J_i} \boldsymbol{\omega}_{qi} = \boldsymbol{\tau}_i \ ,
\end{aligned}
\tag{1}
$$

where $\mathbf{M_q} = m_o \mathbf{I_3} + \sum_{i=1}^{4} m_i \mathbf{q_i} \mathbf{q_i^T}$ . In the above, $\mathbf{a}^{\times} \in \mathbb{R}^{3\times 3}$ is a skew-symmetric cross-product matrix of vector $\mathbf{a} \in \mathbb{R}^{3\times 1}$. Moreover, $\mathbf{p}_o \in \mathbb{R}^3$ is the position of payload in the inertial frame, while $\boldsymbol{\omega}_o \in \mathbb{R}^3$, $\boldsymbol{\omega}_i \in \mathbb{R}^3$ and $\boldsymbol{\omega}_{qi} \in \mathbb{R}^3$ are the angular velocities of the payload in its body frame (here, the payload body frame is named as $\mathbb{B}$), the $i$th link in the inertial frame, and the $i$th drone in its own body frame, respectively. In addition, $m_o$, $m_i$, $l$, $\mathbf{J}_o \in \mathbb{R}^{3\times 3}$ and $\mathbf{J}_i \in \mathbb{R}^{3\times 3}$ are mass of the payload, mass of the $i$th drone, length of each link (assumed the same for all links), the centroidal inertia matrix of the payload and the inertia matrix of the $i$th drone around its corresponding center of mass, respectively. Here, $\boldsymbol{\rho}_i \in \mathbb{R}^3$ locates the joint of the $i$th link on the payload with respect to its center of mass in $\mathbb{B}$. Moreover, $\mathbf{R_o} \in \mathbb{R}^{3\times 3}$ transforms vector components from the payload body frame $\mathbb{B}$ to inertial frame, and $\mathbf{G} = [0, 0, g_e]^T$ is the gravity vector in inertial frame (NED frame is considered). The variable $\mathbf{q}_i \in \mathbb{R}^3$ is the unit vector of the $i$th link in the inertial frame, as shown in Fig. 1. The system inputs include the generated torque at the $i$th drone $\boldsymbol{\tau}_i \in \mathbb{R}^3$ (defined in the body frame of the $i$th drone) and the transmitted force to the $i$th link from the $i$th drone, i.e. $\mathbf{u_i} \in \mathbb{R}^3$. In the latter category, each force is divided into components parallel to the $i$th link, $\mathbf{u_i^{\parallel}} \in \mathbb{R}^3$ and perpendicular to the $i$th link, $\mathbf{u_i^{\perp}} \in \mathbb{R}^3$ (all defined in the inertial frame). Following [8] and [9], the parallel and perpendicular projections of the total input force on the $i$th link are defined as follows ($\mathbf{I_3} \in \mathbb{R}^3$ is an identity matrix)

$$
\mathbf{u_i^{\parallel}} = \mathbf{q}_i \mathbf{q}_i^T \mathbf{u_i} \quad , \quad \mathbf{u_i^{\perp}} = (\mathbf{I_3} - \mathbf{q}_i \mathbf{q}_i^T) \mathbf{u_i} \ , \tag{2}
$$

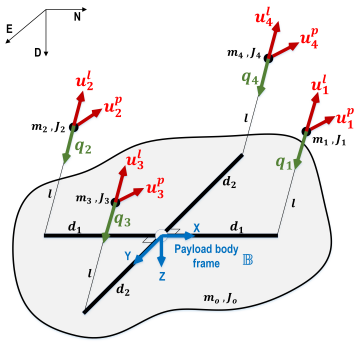


Fig. 1: Schematic of the system with four drones and four rigid links lifting a rigid payload. The arrangement of joint locations is also shown in the payload body frame $\mathbb{B}$.

**Assumption-1**. According to Fig. 1, there are four joints on the payload via which the links are connected to the payload. By considering two virtual connecting lines between the joints to drone-1 and drone-2 as well as the joints to drone-3 and drone-4, it is assumed that these two lines are perpendicular and their conjunction point is the center of mass of the payload. In light of the aforementioned assumptions, we have $\boldsymbol{\rho_1} = [d_1, 0, 0]^T$, $\boldsymbol{\rho_2} = [-d_1, 0, 0]^T$, $\boldsymbol{\rho_3} = [0, d_2, 0]^T$ and $\boldsymbol{\rho_4} = [0, -d_2, 0]^T$.

**Assumption-2**. It is assumed that each of the links can rotate around two directions normal to itself, while it does not rotate around its axis, i.e., $\boldsymbol{\omega}_i^T \mathbf{q}_i = 0$. Moreover, it is assumed that each link is connected to the center of mass of the corresponding quadrotor using a universal joint.

**Proposition-1**. The payload transport problem considered here bears similarities to a cable parallel robot system. In the latter, the links must be always in tension and the objective is to control the motion of the payload in six degrees of freedom [10], [11], [12], as is the case in the current problem. On the other hand, in a cable parallel robot, the link lengths are variable, while the actuators driving the cables are fixed in space. Thus, the actuators generate forces to control the lengths of the cables in order to regulate the position and orientation of the payload. In contrast, in the collaborative payload transport scenario, the link lengths are fixed, while

the system "actuators"—the quadrotors—are free to move in space. Our goal is to control the quadrotors which in turn control the links' orientations so that the payload tracks its desired motion. An in-depth analysis of the existence of solution to this problem is presented in [13].

## III. Design of Control Architecture and Observer

**Proposition-2**. A swing-free motion of the payload can be achieved if its position tracks the desired trajectory, while its attitude remains constant. In other words, the swing-free motion would be provided if the tracking error

$$\mathbf{e} = \mathbf{x}_o^d - \mathbf{x}_o \ , \tag{3}$$

is bounded within a small area around the origin, where $\mathbf{x}_o = [\mathbf{p}_o^T, \mathbf{\Phi}_o^T]^T \in \mathbb{R}^{6\times 1}$ includes position $\mathbf{p}_o = [x_o, y_o, z_o]^T$ and attitude coordinates $\mathbf{\Phi}_o = [\phi_o, \theta_o, \psi_o]^T$ of the payload, and $\mathbf{x_o^d} \in \mathbb{R}^{6\times 1}$ is the corresponding desired variable.

**Proposition-3**. The control problem is to design control inputs to each of the aerial mobile robots, so as to provide a swing-free tracking motion of the payload, while maintaining a desired formation topology between the drones.

**Proposition-4**. The proposed control architecture for motion tracking of the payload and formation maintenance among the drones is depicted in Fig. 2. The desired set-points for position and orientation of the payload are converted to the desired translational and angular velocities of the payload, using two proportional controllers on the corresponding tracking errors with gains $k_p > 0$ and $k_a > 0$, respectively. Then, the AMFC-1 and AMFC-2 modules (AMFC is defined in *Lemma-1*) are implemented on the desired velocity set-points of the payload and produce the desired translational and angular acceleration of the payload, i.e., $\mathbf{X^d}$. The desired acceleration set-points are fed into the pseudo-inverse (PINV) module (presented in *Lemma-2* with extension in *Lemma-3*). The PINV module is responsible for determining the desired force to be applied by each link on the payload (i.e., $\boldsymbol{\mu_i^d}$ in (12)). Furthermore within the PINV module, the desired unit vector of each link ($\mathbf{q_i^d}$ in (13)) as well as the desired magnitude of the force along it ($f_i^d$ in (13)) are computed. Then, a proportional controller with gain $k_q > 0$ is utilized to convert the attitude error of each link to its desired attitude rate. This is followed by using the AMFC-3 module to determine the required perpendicular control inputs $\mathbf{u_i}^{\perp}$ at each link, which in-turn are combined with the desired parallel control inputs $\mathbf{u_i}^{\parallel}$ to generate the resultant forces required at each drone, as follows

$$\mathbf{u_i} = \mathbf{u_i}^{\parallel} + \mathbf{u_i}^{\perp} \ . \tag{4}$$

The values for $\hat{\mathbf{q}}_i$ and $\hat{\dot{\mathbf{q}}}_i$ are estimated using the linear Kalman filter proposed in *Lemma-4*. In addition, by assuming $\psi_i^d = 0$ and using the following transformation [15]

$$\phi_i^d = \arctan\frac{\mathbf{u_i}(2)}{T_i} \quad , \quad \theta_i^d = \arctan\frac{\mathbf{u_i}(1)}{\mathbf{u_i}(3)} \ , \tag{5}$$

where $T_i = |\mathbf{u_i}|$ is the required thrust force at the $i$th drone, the desired attitude $\mathbf{\Phi_i^d} = [\phi_i^d, \theta_i^d, \psi_i^d]^T$ at each drone is defined [16]. Finally, the desired attitude would be satisfied at each drone, by incorporating the AMFC-4 module.

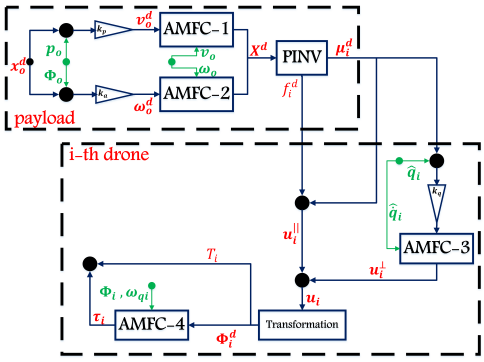


Fig. 2: Flowchart of the control scheme. AMFC-1: translational velocity controller of payload; AMFC-2: angular velocity controller of payload; AMFC-3: controller for rate of unit vector at each link; AMFC-4: attitude controller of each quadrotor. PINV module is responsible for determining desired unit vector and force along each link.

**Lemma-1**. The major element of the proposed control structure is the adaptive model-free control (AMFC) algorithm (proposed in [14], [15]) for tracking the desired linear and angular velocities of the payload, the rates $\dot{\mathbf{q}}_i$ of each link in the system, and the attitude of each quadrotor. For a generic dynamic system defined with:

$$\dot{\mathbf{x}} = \mathbf{A}\mathbf{x} + \mathbf{B}\mathbf{u} + \mathbf{g} \ , \tag{6}$$

with unknown linearities $\mathbf{A} \in \mathbb{R}^{n\times n}$ and unknown nonlinearities $\mathbf{g} \in \mathbb{R}^n$ ($n$ is the number of system states), the AMFC is defined as follows [14]

$$\begin{aligned}
&\mathbf{u} = \mathbf{B}^{-1}[\dot{\mathbf{x}}_\mathbf{d} - \hat{\mathbf{A}}\mathbf{x} - \hat{\mathbf{g}} - \boldsymbol{\zeta} + (\mathbf{I_n} + 2\mathbf{P}^{-1}\mathbf{Q} + \hat{\mathbf{A}})\boldsymbol{\sigma}] - \frac{1}{4}\mathbf{R}\mathbf{B}^T\mathbf{P}\boldsymbol{\sigma} \ , \\
&\dot{\mathbf{P}} = \hat{\mathbf{A}}^T\mathbf{P} + \mathbf{P}\hat{\mathbf{A}} - \mathbf{P}\mathbf{B}\mathbf{R}\mathbf{B}^T\mathbf{P} + 2\mathbf{Q} \ , \\
&\dot{\hat{\mathbf{g}}} = -\gamma_1\mathbf{P}\boldsymbol{\sigma} - \beta_1\gamma_1\hat{\mathbf{g}} \ , \\
&\boldsymbol{\nu}_{\hat{\mathbf{A}}} = -\gamma_2\mathbf{P}\mathbf{M}_{\boldsymbol{\sigma}}(\mathbf{x} - \boldsymbol{\sigma}) - \beta_2\gamma_2\boldsymbol{\nu}_{\hat{\mathbf{A}}} \ .
\end{aligned} \tag{7}$$

Here, $\boldsymbol{\zeta} = \int_0^t \mathbf{e}dt \in \mathbb{R}^n$, $\boldsymbol{\sigma} = \mathbf{e} + \boldsymbol{\zeta}$, $\mathbf{I_n} \in \mathbb{R}^{n\times n}$ is an identity matrix, while $\mathbf{R}$, $\mathbf{Q}$, $\gamma_1$, $\gamma_2$ all in $\mathbb{R}^{n\times n}$ and the positive scalars $\beta_1$ and $\beta_2$, are the tuning parameters of the AMFC. In addition, $\boldsymbol{\nu}_{\hat{\mathbf{A}}} \in \mathbb{R}^n$ is a vector whose elements are the diagonal elements of $\hat{\mathbf{A}}$; and $\mathbf{M}_{\boldsymbol{\sigma}} \in \mathbb{R}^{n\times n}$ is a diagonal matrix whose diagonal values are the elements of vector $\boldsymbol{\sigma}$.

**Definition-2**. The dynamics equations of the payload, separated from the connecting links are:

$$\begin{aligned}
\mathbf{J}_o\dot{\boldsymbol{\omega}}_o + \boldsymbol{\omega}_o^{\times}\mathbf{J}_o\boldsymbol{\omega}_o &= \sum_{i=1}^{4}\boldsymbol{\rho}_i^{\times}\mathbf{R}_o^T\boldsymbol{\mu}_i \ , \\
m_o\ddot{\mathbf{p}}_o - m_o\mathbf{G} &= \sum_{i=1}^{4}\boldsymbol{\mu}_i \ ,
\end{aligned} \tag{8}$$

where $\boldsymbol{\mu_i} = -f_i\mathbf{q_i}$ are the forces applied by the links to the payload. Here, $f_i$ (for $i \in \{1, 2, 3, 4\}$) is the magnitude of

force applied to the payload by the $i$th link. Rewriting (8) in matrix form gives:

$$\mathbf{X} = \mathbf{B}\boldsymbol{\mu} + \mathbf{D} \,, \tag{9}$$

where $\mathbf{X} = [\ddot{x}_o, \ddot{y}_o, \ddot{z}_o, \dot{\omega}_x, \dot{\omega}_y, \dot{\omega}_z] \in \mathbb{R}^{6\times 1}$ is the vector of angular and linear accelerations of the payload, $\boldsymbol{\mu} = [\boldsymbol{\mu_1}^T, \boldsymbol{\mu_2}^T, \boldsymbol{\mu_3}^T, \boldsymbol{\mu_4}^T]^T \in \mathbb{R}^{12\times 1}$ is the vector of all forces exerted on the payload by the links, $\mathbf{D} = [\mathbf{G}^T, (-\mathbf{J}_o^{-1}(\boldsymbol{\omega}_o^{\times}\mathbf{J}_o\boldsymbol{\omega}_o))^T]^T \in \mathbb{R}^{6\times 1}$, and

$$\mathbf{B} = \begin{bmatrix} \frac{1}{m_o}\mathbf{I_3} & \frac{1}{m_o}\mathbf{I_3} & \frac{1}{m_o}\mathbf{I_3} & \frac{1}{m_o}\mathbf{I_3} \\ \mathbf{J}_o^{-1}\boldsymbol{\rho}_1^{\times}\mathbf{R}_o^T & \mathbf{J}_o^{-1}\boldsymbol{\rho}_2^{\times}\mathbf{R}_o^T & \mathbf{J}_o^{-1}\boldsymbol{\rho}_3^{\times}\mathbf{R}_o^T & \mathbf{J}_o^{-1}\boldsymbol{\rho}_4^{\times}\mathbf{R}_o^T \end{bmatrix} . \tag{10}$$

Note that $\mathbf{B} \in \mathbb{R}^{6\times 12}$ is full-rank. Moreover, introducing $\mathbf{Z} = \mathbf{X} - \mathbf{D}$, leads to the following compact matrix equation:

$$\mathbf{B}\boldsymbol{\mu} = \mathbf{Z} \,. \tag{11}$$

Since $\mathbf{B}$ is full-rank [8], $\mathbf{B}\mathbf{B}^T$ is invertible and there is at least one solution for $\boldsymbol{\mu}$ in (11).

**Lemma-2**. Based on *Definition-2*, in order to provide the desired acceleration of the payload $\mathbf{X}^d$, the desired forces applied to the payload, i.e., $\boldsymbol{\mu}^d = [\boldsymbol{\mu_1^d}^T, \boldsymbol{\mu_2^d}^T, \boldsymbol{\mu_3^d}^T, \boldsymbol{\mu_4^d}^T]^T$ are computed by the PINV module as follows:

$$\boldsymbol{\mu^d} = \mathbf{B}^T(\mathbf{B}\mathbf{B}^T)^{-1}\mathbf{Z^d} \,, \tag{12}$$

which is the minimum-norm solution of the matrix equation (11) and $\mathbf{Z^d} = \mathbf{X^d} - \mathbf{D}$. With the values of $\boldsymbol{\mu_i^d}$ as per (12) and recalling $\boldsymbol{\mu_i} = -f_i\mathbf{q_i}$, one can determine the desired force along the $i$th link, $f_i^d$, and also the desired values for the corresponding orientation unit vector $\mathbf{q}_i^d$ as follows:

$$f_i^d = |\boldsymbol{\mu_i^d}| \quad , \quad \mathbf{q_i^d} = \frac{-\boldsymbol{\mu_i^d}}{f_i^d} \,. \tag{13}$$

**Remark-1**. Utilizing *Lemma-2*, the desired orientations of all links are defined to ensure the desired forces at the corresponding joints are transmitted to the payload. This leads to the motions of the drones, while the desired relative positions among them are not considered. In other words, *Lemma-2* does not provide control of the drones' formation and hence the collision avoidance between them is not guaranteed.

**Proposition-5**. Inspired by the nature of the translational motion control of an under-actuated quadrotor, and referring to Fig. 1, we propose that drone-1 and drone-2 be responsible for the translational motion of the payload along the x-axis of $\mathbb{B}$, while drone-3 and drone-4 be responsible for the translational motion of the payload along the y-axis of $\mathbb{B}$. In addition, we assume that the desired attitude of the payload is set such that $\mathbb{B}$ is aligned with NED frame (i.e., zero rotations). Moreover, all drones contribute to the payload translation in $z$ direction of $\mathbb{B}$.

**Proposition-6** The approach in *Proposition-5* helps to define a set of desired orientations of the links for achieving the desired relative positions between the drones in $\mathbb{B}$. These desired link orientations have to be defined. Specifically, by defining $\mathbf{q_i^o} = \mathbf{R_o}^T\mathbf{q_i}$, one can set $\mathbf{q_1^o}(2) = \mathbf{q_2^o}(2)$ and $\mathbf{q_1^o}(1) = -\mathbf{q_2^o}(1)$, in order to provide a desired relative distance between drone-1 and drone-2 in the x-axis of $\mathbb{B}$ (see Fig. 3). With this configuration, the force components generated by link-1 and link-2 along the x-axis of $\mathbb{B}$ would eliminate each other, while the summation of components of these forces along y-axis of $\mathbb{B}$ can provide the required force for translational motion of the payload along this axis. Similarly with the same assumptions, by setting $\mathbf{q_3^o}(1) = \mathbf{q_4^o}(1)$ and $\mathbf{q_3^o}(2) = -\mathbf{q_4^o}(2)$, the force components generated by link-3 and link-4 in the y-axis of $\mathbb{B}$ are eliminated, while a desired relative distance in that axis is achieved among drone-3 and drone-4. The summation of the the first components of the forces applied by link-3 and link-4, provides the desired motion of the payload along x-axis of $\mathbb{B}$.

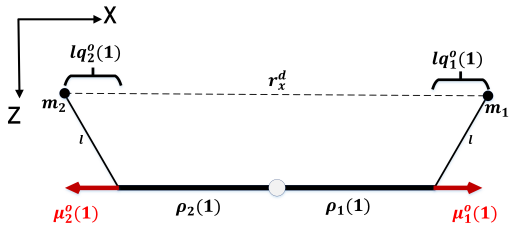


Fig. 3: Configuration of link-1 and link-2 for satisfying the desired relative position between drone-1 and drone-2 in the payload body frame $\mathbb{B}$.

**Lemma-3**. Recalling *Proposition-6* for maintaining a desired formation topology among the drones, the suggested configurations for the orientation of links can be achieved by defining four constraints on the orientations of the links and incorporating them into the matrix equation in (11). The first two constraints are simply the equality of the specified force components in $\mathbb{B}$, as follows:

$$\boldsymbol{\mu_1^o}(1) + \boldsymbol{\mu_2^o}(1) = 0 \quad , \quad \boldsymbol{\mu_3^o}(2) + \boldsymbol{\mu_4^o}(2) = 0 \,, \tag{14}$$

where $\boldsymbol{\mu_i^o} = \mathbf{R_o}^T\boldsymbol{\mu_i}$. The second two constraints are defined to relate the desired relative distances to the force components. In this regard, one can define

$$\boldsymbol{\mu_1^o}(1) = -f_1\mathbf{q_1^o}(1) = k_1 \ , \ \boldsymbol{\mu_3^o}(2) = -f_3\mathbf{q_3^o}(2) = k_2 \,. \tag{15}$$

Besides, from the geometry depicted in Fig. 3, one can have

$$2l\mathbf{q_1^o}(1) + 2|\boldsymbol{\rho_1}(1)| = r_x^d \quad , \quad 2l\mathbf{q_3^o}(2) + 2|\boldsymbol{\rho_3}(2)| = r_y^d \,. \tag{16}$$

Thus, by substituting for $\mathbf{q_1^o}(1)$ and $\mathbf{q_3^o}(2)$ from (16) into respective equations in (15), it leads to

$$f_1 = \frac{-k_1}{h_1} \quad , \quad f_3 = \frac{-k_2}{h_2} \,, \tag{17}$$

where

$$h_1 = \frac{r_x^d - 2|\boldsymbol{\rho_1}(1)|}{2l} \quad , \quad h_2 = \frac{r_y^d - 2|\boldsymbol{\rho_3}(1)|}{2l} \,. \tag{18}$$

In the above, $r_x^d$ and $r_y^d$ are the desired relative distances between drones in x and y directions of $\mathbb{B}$. Moreover, $f_1$ and $f_3$ are defined by utilizing (13) as follows

$$\begin{aligned} f_1 &= \sqrt{(k_1)^2 + (\mathbf{Z^o}(2)/2)^2 + (\mathbf{Z^o}(3)/4)^2} \,, \\ f_3 &= \sqrt{(\mathbf{Z^o}(1)/2)^2 + (k_2)^2 + (\mathbf{Z^o}(3)/4)^2} \,, \end{aligned} \tag{19}$$

where $\mathbf{Z^o} = m_o {\mathbf{R_o}}^T[\mathbf{Z}(1), \mathbf{Z}(2), \mathbf{Z}(3)]^T$, by recalling the first three rows of $\mathbf{B}$ from (10). In (19), $\boldsymbol{\mu}^o_{\mathbf{1}}(1)$ and $\boldsymbol{\mu}^o_{\mathbf{3}}(2)$ are replaced from (15), while the rest of force components are replaced based on the fact that the solution in (12) is a minimum-norm solution and each link is responsible for the equal share of the total requested force components on the payload. By replacing $f_1$ and $f_3$ from (17) into (19), the values for $k_1$ and $k_2$ are determined using:

$$k_1 = -\sqrt{\frac{(\mathbf{Z^o}(2)/2)^2 + (\mathbf{Z^o}(3)/4)^2}{\frac{1}{h_1^2} - 1}} \ , \\ k_2 = -\sqrt{\frac{(\mathbf{Z^o}(1)/2)^2 + (\mathbf{Z^o}(3)/4)^2}{\frac{1}{h_2^2} - 1}} \ . \tag{20}$$

Furthermore, by considering the constraints defined in (14) and (15), the matrix equation in (6) is updated as follows

$$\mathbf{B}_{ext}\ \boldsymbol{\mu} = \mathbf{Z}_{ext} \ , \tag{21}$$

where $\mathbf{B}_{ext} = [\mathbf{B}; \mathbf{B_t}] \in \mathbb{R}^{10\times 12}$ for

$$\mathbf{B_t} = \begin{bmatrix} \mathbf{b_x} & \mathbf{b_x} & \mathbf{n}_6 \\ \mathbf{n}_6 & \mathbf{b_y} & \mathbf{b_y} \\ \mathbf{b_x} & \mathbf{n}_3 & \mathbf{n}_6 \\ \mathbf{n}_6 & \mathbf{b_y} & \mathbf{n}_3 \end{bmatrix} \in \mathbb{R}^{4\times 12} \ , \tag{22}$$

$\mathbf{b_x} = ({\mathbf{R_o}}^T[1,0,0]^T)^T$, $\mathbf{b_y} = ({\mathbf{R_o}}^T[0,1,0]^T)^T$, $\mathbf{n}_3 = [0,0,0]$, $\mathbf{n}_6 = [0,0,0,0,0,0]$, and $\mathbf{Z}_{ext} = [\mathbf{Z}^T, 0, 0, k_1, k_2]^T \in \mathbb{R}^{10\times 1}$. Then, similar to (12), the solution for $\boldsymbol{\mu^d}$ is defined as follows

$$\boldsymbol{\mu^d} = \mathbf{B}_{ext}^T(\mathbf{B}_{ext}\mathbf{B}_{ext}^T)^{-1}\mathbf{Z^d}_{ext} \ , \tag{23}$$

and equations in (13) are used to determine $f_i^d$ and $\mathbf{q_i^d}$.

**Remark-2**. According to (20) and (18), the desired distances between drones 1 and 2 as well as drones 3 and 4,must satisfy the following constraints

$$0 < r_x^d < 2(d_1 + l) \quad , \quad 0 < r_y^d < 2(d_2 + l) \ . \tag{24}$$

Recalling Fig. 1 and *Assumption-1*, $2(d_1 + l)$ and $2(d_2 + l)$ are the maximum achievable distances between drone-1 to drone-2 and drone-3 to drone-4, respectively.

**Remark-3**. According to the proposed control scheme in Fig. 2, the orientation of each link $\mathbf{q}_i$ and its first time-derivative are required for generating the desired values of $\mathbf{u_i}^{\parallel}$ and $\mathbf{u_i}^{\perp}$ at each drone. The values of $\mathbf{q}_i$ and $\dot{\mathbf{q}}_i$ need to be estimated by a suitable observer algorithm, in the absence of on-board sensors to measure them.

**Lemma-4**. As mentioned previously, each $\mathbf{q}_i$ is defined with respect to the inertial frame. Hence, the absolute position of drone $i$ is represented as follows:

$$\mathbf{p}_i = \mathbf{p}_o + \mathbf{R}_o\boldsymbol{\rho}_i - l\mathbf{q}_i \ . \tag{25}$$

and by rearranging (25), one obtains:

$$\mathbf{q}_i = \frac{1}{l}(\mathbf{p}_o - \mathbf{p}_i) + \frac{1}{l}\mathbf{R}_o\boldsymbol{\rho}_i = \mathbf{y}^i_{ob} \ . \tag{26}$$

Besides, the second-derivative of equation in (25) with respect to time is computed as follows

$$\ddot{\mathbf{p}}_i = \ddot{\mathbf{p}}_o + \mathbf{R}_o\boldsymbol{\omega}_o^{\times}\boldsymbol{\omega}_o^{\times}\boldsymbol{\rho}_i + \mathbf{R}_o\dot{\boldsymbol{\omega}}_o^{\times}\boldsymbol{\rho}_i - l\ddot{\mathbf{q}}_i \ . \tag{27}$$

and by rearranging (27):

$$\ddot{\mathbf{q}}_i = \frac{1}{l}(\ddot{\mathbf{p}}_o - \ddot{\mathbf{p}}_i) + \frac{1}{l}\mathbf{R}_o\boldsymbol{\omega}_o^{\times}\boldsymbol{\omega}_o^{\times}\boldsymbol{\rho}_i + \frac{1}{l}\mathbf{R}_o\dot{\boldsymbol{\omega}}_o^{\times}\boldsymbol{\rho}_i = \mathbf{u}^i_{ob} \ . \tag{28}$$

Accordingly, the kinematics of the $i$th link can be represented by the following linear state-space system

$$\dot{\mathbf{x}}^i_{ob} = \mathbf{A}_{ob}\mathbf{x}^i_{ob} + \mathbf{B}_{ob}\mathbf{u}^i_{ob} \ , \\ \mathbf{y}^i_{ob} = \mathbf{C}_{ob}\mathbf{x}^i_{ob} \ , \tag{29}$$

in which $\mathbf{x}^i_{ob} = [\mathbf{q}_i^T, \dot{\mathbf{q}}_i^T]^T$, and

$$\mathbf{A}_{ob} = \begin{bmatrix} \mathbf{0}_3 & \mathbf{I}_3 \\ \mathbf{0}_3 & \mathbf{0}_3 \end{bmatrix} \ , \ \mathbf{B}_{ob} = \begin{bmatrix} \mathbf{0}_3 \\ \mathbf{I}_3 \end{bmatrix} \ , \ \mathbf{C}_{ob} = \begin{bmatrix} \mathbf{I}_3 & \mathbf{0}_3 \end{bmatrix} \ . \tag{30}$$

Finally, a linear Kalman-filter is implemented on the dynamics and measurement models presented in (29).

**Remark-4**. To compute the values for $\mathbf{y}^i_{ob}$, the relative position of the $i$th drone with respect to the payload is required. This relative position can be measured by using cameras mounted on the drones looking toward a fiducial marker affixed to the payload. Alternatively, one can use the relative position estimation algorithm presented in [17].

**Remark-5**. To determine the values for $\mathbf{u}^i_{ob}$, the relative acceleration of the $i$th drone with respect to the payload, the angular velocity and the angular acceleration of the payload are required. The relative acceleration between each of the drones and the payload is determined by transmitting the measured acceleration of the payload to the corresponding drone. The angular velocity and acceleration of the payload is estimated by on-board IMU mounted on the payload.

## IV. Simulation Results

We present simulation results to validate the proposed controller and observer schemes. The specifications of the system are as follows: $m_o = 5$kg, $\mathbf{J_o}$ =diag($[0.83, 0.83, 0.83]$)kg-m$^2$, $d_1 = d_2 = 1$m and $l = 2$m. For the drones, $m_i = 1$kg and $\mathbf{J_i}$ =diag($[0.08, 0.08, 0.14]$)kg-m$^2$ for $i = \{1, 2, 3, 4\}$. The desired distances between the drones are defined as $r_x^d = r_y^d = 3$m, while the reference trajectory for the payload is $\mathbf{p_o^d} = [1.2\sin(0.2\pi t), 4.2\cos(0.1\pi t), -0.5]^T$. The reference attitude of the payload is zero in NED frame. In addition, the variance of measurement noise is set to $\sigma_p = 10$mm for the relative position and $\sigma_a = 10$mm/$s^2$ for the relative acceleration measurements between the drones and the payload. Here, it is assumed that the noise amplitudes on angular velocity and angular acceleration of the payload are very low after filtering method as in [18]). The tuned parameters of the proposed solution are presented in Table I. As can be seen, minimal effort is required to tune the gains. Simulation results are provided in Figs. 4-10. The reference 3D trajectory is tracked by the payload properly, as seen in Fig. 4. Also, the largest deviation in Euler angles of the payload is 0.02rad (refer to Fig. 5). This leads to bounded tracking error for payload translational and rotational motions, defined by $\mathbf{e}$ in (3). Performance of the proposed observer is validated, according to Figs. 6 and 7. Moreover, the desired relative positions among the drones are achieved in inertial frame, as seen in Figs. 9 and 10, with bounded generated torques at vehicles confirmed in Fig. 8.

TABLE I: Tuned parameters of controllers

| | | |
|---|---|---|
| $k_p = 1$ | $k_a = 1$ | $k_q = 10$ |
| **AMFC-1** | | |
| $\mathbf{Q} = \mathbf{R} = \mathbf{I_3}$ | $\boldsymbol{\gamma_1} = \boldsymbol{\gamma_2} = 10^3 \times \mathbf{I_3}$ | $\beta_1 = 1, \beta_2 = 0.001$ |
| **AMFC-2** | | |
| $\mathbf{Q} = \mathbf{R} = \mathbf{I_3}$ | $\boldsymbol{\gamma_1} = \boldsymbol{\gamma_2} = 10^3 \times \mathbf{I_3}$ | $\beta_1 = \beta_2 = 1$ |
| **AMFC-3** | | |
| $\mathbf{Q} = \mathbf{R} = \mathbf{I_3}$ | $\boldsymbol{\gamma_1} = \boldsymbol{\gamma_2} = 0.01 \times \mathbf{I_3}$ | $\beta_1 = \beta_2 = 1$ |
| **AMFC-4** | | |
| $\mathbf{Q} = \mathbf{R} = \mathbf{I_6}$ | $\boldsymbol{\gamma_1} = \boldsymbol{\gamma_2} = [\mathbf{I_3}; 10^3 \times \mathbf{I_3}]$ | $\beta_1 = \beta_2 = 1$ |

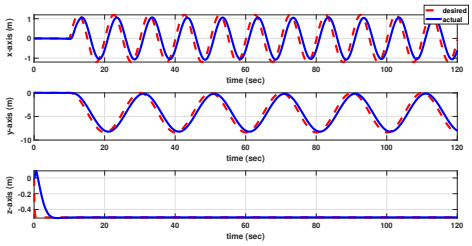


Fig. 4: Actual and desired position of payload

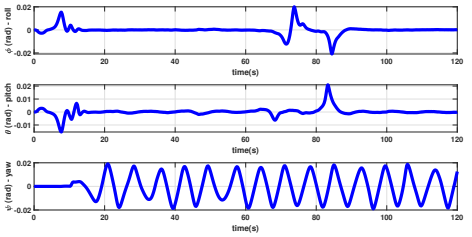


Fig. 5: Orientation of payload

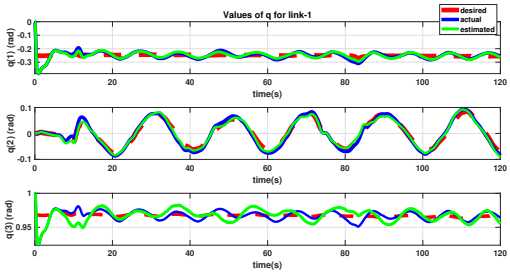


Fig. 6: Desired, actual and estimated components of $\mathbf{q}_1$

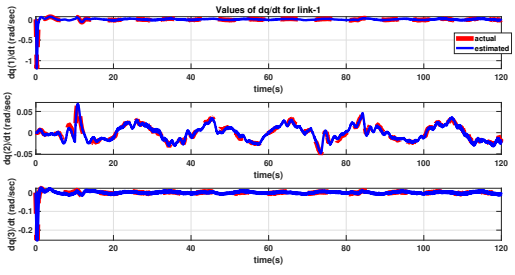


Fig. 7: Actual and estimated components of $\dot{\mathbf{q}}_1$

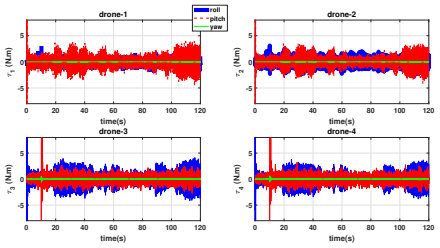


Fig. 8: Torques generated by the drones

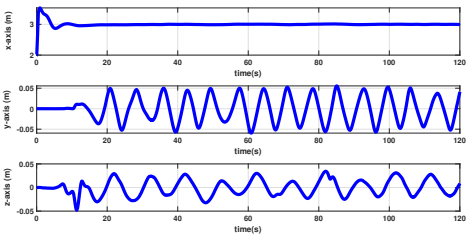


Fig. 9: Relative position of drone-1 w.r.t drone-2

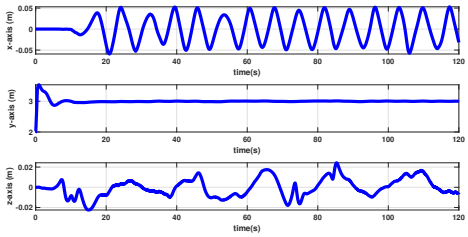


Fig. 10: Relative position of drone-3 w.r.t drone-4

## V. Conclusion

In this paper, a novel controller-observer formulation is proposed for the problem of collaborative transportation of a payload by four quadrotors. The control problem is divided into four modules: the translational and rotational motions of the payload, rotational motion of each connecting link and the rotational motion of each quadrotor. Adaptive model-free control algorithm is employed for each module, removing the requirement for information on the internal dynamics of the quadrotors. The desired formation topology among the quadrotors is maintained by incorporating a pseudo-inverse solution of a generalized linear matrix equation for the payload's dynamics. In addition, a specific linear Kalman-filter is suggested for estimating the direction of each connecting link and its rate of change. Simulation results demonstrate good position tracking for the payload is achieved, while a desired formation among the drones is maintained.


## Acknowledgment

This research was conducted under a Mitacs Accelerate program at McGill University and HumanITAS Solutions. Support through the NSERC Canadian Robotics Network (NCRN) is also acknowledged

## REFERENCES


[1] R. Costakis, D. St-Onge and G. Beltrame, "Decentralized collaborative transport of fabrics using micro-UAVs," in proceedings of *2019 International Conference on Robotics and Automation*, Montreal, Canada, pp. 7734-7740, 2019.

[2] J. Gimenez, D. Gandolfo, L. Salinas, C. Rosales and R. Carelli, "Multi-objective control for cooperative payload transport with rotorcraft UAVs," *ISA Transactions*, vol. 80, pp. 491-502, 2018.

[3] K. Klausen, T Fossen, T Johansen and A. Aguiar, "Cooperative path-following for multirotor UAVs with a suspended payload," in proceedings of *2015 IEEE Conference on Control and Applications*, Sydney, Australia, 1354-1360, 2015.

[4] K. Sreenath and V. Kumar, "Dynamics, control and planning for cooperative manipulation of payloads suspended by cables from multiple quadrotor robots," in proceedings of *Robotics: Science and Systems*, 2013; 10.15607/rss.2013.ix.011.

[5] I. Pizetta, A. Brandao and M. Sarcinelli-Filho, "Cooperative quadrotors carrying a suspended load," in proceedings of *2016 Int. Conference on Unmanned Aircraft Systems*, Arlington, VA, pp. 1049-1055, 2016.

[6] Y.H. Tan, S. Lai, K. Wang and B.M. Chen, "Cooperative heavy lifting using unmanned multi-agent systems," in proceedings of *2018 IEEE 14th International Conference on Control and Automation*, Anchorage, Alaska, pp. 1119-1126, 2018.

[7] S. Thapa, H. Bai and J.A. Acosta, "Cooperative aerial manipulation with decentralized adaptive force-consensus control," *Journal of Intelligent and Robotic Systems*, vol. 97, pp. 171-183, 2020.

[8] T. Lee, "Geometric control of multiple quadrotor UAVs transporting a cable-suspended rigid body", in *53rd IEEE Conference on Decision and Control*, LA, California, pp. 6155-6160, 2014.

[9] T. Lee, "Geometric control of quadrotor UAVs transporting a cable-suspended rigid body", *IEEE Transactions on Control Systems Technology,* Vol. 26, No. 1, pp. 255-264, 2018.

[10] A. Trevisani, "Underconstrained planar cable-direct-driven robots: A trajectory planning method ensuring positive and bounded cable tensions," *Mechatronics*, vol. 20, pp. 113-127, 2010.

[11] D.Q. Nguyen, M. Gouttefrade, O. Company and F. Pierrot, "On the analysis of large-dimension reconfigurable suspended cable-driven parallel robots," in proceedings of *2014 IEEE International Conference on Robotics and Automation*, Hong Kong, pp. 5728-5735, 2014.

[12] L. Gagliardini, S. Caro, M. Gouttefarde and A. Girin, "Discrete reconfiguration planning for cable-driven parallel robots," *Mechanism and Machine Theory*, vol. 100, pp. 313-337, 2016.

[13] J.C. Erskine, A. Chriette and S. Caro, "Wrench analysis of cable-suspended parallel robots actuated by quadrotors UAVs," *ASME Journal of Mechanism and Robotics*, vol. 11, no. 2, pp. 020909-1–020909-12, 2019.

[14] A. Safaei and M. N. Mahyuddin, "Adaptive model-free control based on an ultra-local model with model-free parameter estimations for a generic SISO system," *IEEE Access*, Vol. 6, pp. 4266-4275, 2018.

[15] A. Safaei and M. N. Mahyuddin, "Optimal model-free control for a generic MIMO nonlinear system with application to autonomous mobile robots," *International Journal of Adaptive Control and Signal Processing*, Vol. 32, No. 6, pp.792-815, 2018.

[16] A. Safaei and M. N. Mahyuddin, "Lyapunov-based nonlinear controller for quadrotor position and attitude tracking with GA optimization," in *2016 IEEE Industrial Electronics and Applications Conference*, Kota Kinabalu, pp. 342-347, 2016.

[17] A. Safaei and M.N. Mahyuddin, "Adaptive Cooperative Localization Using Relative Position Estimation for Networked Systems With Minimum Number of Communication Links", *IEEE Access*, vol. 7, pp. 32368 - 32382, 2019.

[18] H. Liu, J. Yang, W. Yi, J. Wang, J. Yang, X. Li, and J. Tan, "Angular velocity estimation from measurement vectors of star tracker," *Applied Optics*, Vol. 51, pp. 3590-3598, 2012.